Title
Vertical and latitudinal variation of the intertropical convergence zone derived using GPS radio occultation measurements

Authors
Basha, Ghouse
Kishore, P
Ratnam, M Venkat
et al.

Publication Date
2015-06-01

DOI
10.1016/j.rse.2015.03.024

Peer reviewed

Remote Sensing of Environment 163 (2015) 262–269

Contents lists available at ScienceDirect

Remote Sensing of Environment

journal homepage: www.elsevier.com/locate/rse

Vertical and latitudinal variation of the intertropical convergence zone derived using GPS radio occultation measurements

Ghouse Basha [a,*], P. Kishore [b], M. Venkat Ratnam [c], T.B.M.J. Ouarda [a,d], Isabella Velicogna [b], Tyler Sutterley [b]

[a] Institute Center for Water and Environment (iWATER), Masdar Institute of Science and Technology, P.O. Box 54224, Abu Dhabi, United Arab Emirates
[b] Department of Earth System Science, University of California, Irvine, CA 92697, USA
[c] National Atmospheric Research Laboratory, Gadanki, Tirupati, India
[d] INRS-ETE, National Institute of Scientific Research, Quebec City (QC) G1K9A9, Canada

ARTICLE INFO

Article history:
Received 14 November 2014
Received in revised form 26 March 2015
Accepted 26 March 2015
Available online 11 April 2015

Keywords:
GPSRO
CHAMP COSMIC
ITCZ
Refractivity
Specific humidity

ABSTRACT

Using GPS radio occultation refractivity data collected over the period of 2002–2013, we present a new method for identification of the intertropical convergence zone (ITCZ). The ITCZ is identified by estimating the maximum in the monthly meridional refractivity and specific humidity field by applying a Gaussian fit at each longitude. The interannual variability and climatology of the ITCZ is presented from 12 years of refractivity data. This new method captures all the general features of ITCZ extent and its variability. We also examine the effects of the ITCZ vertically during different seasons. The ITCZ is observed mostly at eastern Pacific in May month, and it is zonally distributed in the September and October months of each year. The zonal variability is large between lower and higher levels, particularly over the Indian monsoon and western Pacific. The latitudinal difference in the vertical extent between 850 hPa and higher levels is larger during the northern hemisphere (NH) summer than NH winter.

1. Introduction

The intertropical convergence zone (ITCZ) is one of the most noticeable aspects of global circulation. The ITCZ is a zone of low pressure near the equator, where two easterly trade winds originating from the northern hemisphere (NH) and southern hemisphere (SH) converge to form a region of increased convection, cloudiness, and precipitation. A belt of low-level convergence and upper-level divergence with strong upward motion, deep penetrative convection, and frequent cloudiness characterizes the ITCZ. The ITCZ is responsible for most of the precipitation on the Earth with maximum toward 5° north. The strength of the ITCZ is also quite variable in both space and time. The location of ITCZ is well defined over the Pacific and Atlantic regions between 5 and 10°N latitudes and appears occasionally in the western Pacific between 5 and 10°S. Such a strong interhemispheric asymmetry in ITCZ distribution despite the essentially interhemispheric symmetric solar radiation forcing has been puzzling theoreticians for quite a long time.

The ITCZ plays an important role in the atmospheric energy balance (Waliser & Gautier, 1993) and the Earth's climate (Zhang, 1993). The excessive heat absorbed from the surface of Tropical Ocean is transported to the lower troposphere through evaporation then to higher altitudes through convection and released as latent heat. This latent heat plays a major role in driving the low-latitude circulation and in supplying energy to balance the radiative heat losses and fuel the wind systems of middle and high latitudes.

Inside and outside the ITCZ, the fluxes of heat, moisture, momentum, and radiation through the surface of the ocean and in the atmosphere itself differ dramatically. The locations of the ITCZ and monsoon trough play a critical role in determining the flow and the precipitation patterns, the tropical cyclone evolution, and the hydrologic cycle of this region. Thus, the position, structure, and migration of the ITCZ are important in defining and analyzing the Earth's climate on a global scale, and the strength and character of the air-sea coupling on a local and global scale. Therefore, the detection of the ITCZ is very important in several aspects.

Traditionally, the ITCZ has either been identified in terms of time-averaged fields, from the seasonal mean outgoing long-wave radiation (OLR) or, in recent years, in terms of the seasonal mean precipitation (Waliser, Groham, & Gautier, 1993). In addition, the ITCZ can be identified by using visible and infrared satellite observations of high reflective cloud cover (Waliser & Gautier, 1993), by locating the convergence of wind fields (e.g., Žagar, Skok, & Tribbia, 2011; Zheng, Yan, Liu, Tang, & Kurz, 1997), by calculating the relative vorticity structures (e.g., Magnusdottir & Wang, 2008), or by using multiple variable criteria (e.g., Bain et al., 2010). Despite the availability of a number of methods for its identifications, some discrepancies in identifying the ITCZ are mentioned in the literature. In particular, over continents, where the trade winds are not well developed, some methods fail to locate the ITCZ position (Nicholson,

* Corresponding author at: iWater, Masdar Institute of Science and Technology, Masdar City, Abu Dhabi 54224, United Arab Emirates.
E-mail address: mdbasha@gmail.com (G. Basha).

http://dx.doi.org/10.1016/j.rse.2015.03.024
0034-4257/

2009). In addition, cloud clusters are included by westward propagating wave disturbances (Chang, 1970; Reed, 1970) and locally (Holton, Wallace, & Young, 1971), which could affect a proper definition of the ITCZ based on precipitation (Nicholson, 2009). In addition, the accurate detection of ITCZ is highly significant for guiding the model improvements, especially in the vertical and latitudinal variations. The climate models (e.g., Coupled Model Inter-Comparison Project 5 (CMIP5) and even the reanalysis has large errors in simulating the convective system over the ocean such as ITCZ (Li & Xie, 2014). Most of the coupled general circulation models (CGCMs) shows large errors in sea surface temperature and excessive westward extension of the equatorial Pacific cold tongue in comparison to observation. Due to the above-specified problems, most of the studies present only the zonally averaged location of ITCZ for particular regions. GPS observation adds another dimension to observe the ITCZ. Especially since the GPSRO, technique requires no active calibration; the data have the potential to be used to study variations and trends of ITCZ in the changing climate.

This paper is a presentation of a simple method to identify the ITCZ from global positioning system (GPS) radio occultation (RO) measurements of Challenging Minisatellite Payload (CHAMP) and Constellation Observing System for Meteorology, Ionosphere, and Climate (COSMIC) refractivity data. In the present study, we extend its detection using a more robust method and provide the climatology of ITCZ using the complete GPSRO data available so far. Further, the effect of the ITCZ up to the 100 hPa is investigated. This study is organized as follows: The data description used in this study is discussed in Section 2. The method of identification the ITCZ is presented in Section 3. In Section 4, the climatology and the variability of the humidity and refractivity distribution characteristics and potential connections to the ITCZ are presented. Finally, conclusive remarks are given in Section 5.

2. Data

The GPSRO technique has unique features of high accuracy, precision, high vertical resolution, and no contamination from clouds, no requirement for system calibration, and no instrument drift (Anthes et al., 2008; Kursinski, Hajj, Hardy, Schofield, & Linfield, 1997). The GPSRO satellites receive radio signals passing through Earth's atmosphere from GPS satellites and calculate the bending angle from the phase during occultation events. The bending angle is then converted, using an Abel inversion technique (Sokolovskiy, 2001), into a vertical refractivity profile that depends upon atmospheric density and the partial pressure of water vapor (Bean & Dutton, 1968). COSMIC provides vertical profiles of refractivity with vertical resolution of 0.5 km to 1 km throughout the troposphere. For the present study, we make use of both CHAMP (2002–2008) and COSMIC (2006–2013) refractivity (N) and specific humidity GPSRO data sets.

The CHAMP (Wickert et al., 2001) was launched into an almost circular near polar orbit (inclination = 87.2°) with an initial altitude of 454 km on 15 July 2000. The first occultation measurement was performed on February 11, 2001, and since then, about 150 to 200 occultations per day have been recorded. For the present study, CHAMP data available from January 2002 to September 2008 is used.

The COSMIC satellite system consists of a constellation of six low Earth orbit (LEO) microsatellites and was launched on 15 April 2006 into a circular, 72° inclination orbit at 512-km altitude (Anthes et al., 2008). The daily number of occultation was about 400 during the first few months and increased significantly to about ~2200 recently. The first COSMIC GPSRO provides global data sets of atmospheric parameters (e.g., refractivity, pressure, temperature, etc.) on 21 April 2006. In this study, we used COSMIC data from January 2007 to December 2013. The GPSRO data used in this study is obtained from the University Corporation for Atmospheric Research (UCAR) COSMIC Data Analysis and Archival Center (CDAAC). The CDAAC 1DVar wet retrieval employs the National Center for Environmental Prediction (NCEP)-National Center for Atmospheric Research (NCAR) reanalysis as the first guess field. The present study uses long-term GPSRO specific humidity and refractivity from January 2002 to December 2013. We also make use of NOAA OLR data for the same period.

3. Methodology to identify the ITCZ

In the neutral atmosphere, the atmospheric refractivity, N, is a dimensionless quantity defined as $N = (n - 1) \times 10^6$, where n (unit less) is atmospheric refractive index. N depends mainly on water vapor and temperature gradients in the lower atmosphere and is given by the following equation (Thayer, 1974):

$$N = (n-1) \times 10^6 = 77.6\frac{P}{T} + 3.73 \times 10^5 \frac{e}{T^2}, \quad (1)$$

P (in mbar) is the total atmospheric pressure, T (in K) is the atmospheric temperature, and e (in mb) is the water vapor pressure. Both the dry term (first term in the right-hand side (RHS) of Eq. (1)) and the wet term (second term in the RHS of Eq. (1)) contribute to the atmospheric refractivity, and thus, independent temperature (water vapor pressure) information must be provided in order to retrieve water vapor pressure (temperature) profiles. Healy and Eyre (2000) described in detail the one-dimensional variational assimilation (1D-Var) technique applied to retrieve both temperature and water vapor profiles from vertical profiles of atmospheric refractivity. GPSRO has emerged as a complementary remote-sensing instrument that provides unprecedented measurements of the thermodynamic environment inside and around the thick clouds, heavy precipitation, and hurricane regions in which visible, infrared, and microwave satellite measurements are largely contaminated (Vergados, Mannucci, & Su, 2013). The comparison of COSMIC and radiosonde humidity was reported to be good in earlier studies (Kishore et al., 2011; Rao et al., 2009; Ratnam, Basha, Krishna Murthy, & Jayaraman, 2014; Wang, Liu, & Wang, 2013). Rao et al. (2009) and Kishore et al. (2011) showed the water vapor information from COSMIC satellite is valid up to ~7 km by comparing with radiosonde and different reanalysis data both regionally and globally. The evaluation of the COSMIC specific humidity with global radiosonde observations showed a bias of about −0.012g/kg between 925 and 200 hPa globally (Wang et al., 2013). Ratnam et al. (2014) compared the relative humidity (RH) from COSMIC and Megha Tropiques satellite and showed that COSMIC RH provides accurate information from 850 to 200 hPa. All these studies showed that COSMIC specific humidity compares well with radiosonde, reanalysis, and other satellite data sets. In troposphere, the contribution of water vapor is more in refractivity than temperature (Basha & Ratnam, 2009; Ratnam & Basha, 2010). However, the refractivity data from GPSRO satellite is very accurate from the surface to 40 km. In addition, it includes both temperature and water vapor information. Using limited data, Ratnam and Basha (2010) also demonstrated the use of GPSRO refractivity to locate the ITCZ. Note that changes, which occur in lower troposphere, can significantly appear in refractivity, whereas in upper troposphere temperature controls the refractivity due to less amount of water vapor contribution. Therefore, by using refractivity alone it is possible to identify the ITCZ from surface to upper troposphere, which is the unique parameter available only from GPSRO satellites directly.

In this section, we introduce a simple and robust method to identify the ITCZ location with respect to the resolution of the satellite data by fitting Gaussian functions. This method deduces characteristics of the meridional distribution of specific humidity and refractivity. For each longitude, the peak position, location, and width (full width half-maximum) of the Gaussian is estimated from GPSRO refractivity and specific humidity data grids. The procedure is based on the method of Läderach and Raible (2013) for identifying the ITCZ from ERA-Interim specific humidity and is applied to the GPSRO specific humidity and refractivity data simultaneously.

The data set comprises global specific humidity and refractivity measurements with grid resolution of 2° longitudes × 2° latitudes. As an initial study, we applied this method on the monthly means of specific humidity and the refractive index at different pressure levels excluding the boundary layer to reduce orography effects. The humidity distribution parameters are assessed by fitting a Gaussian function (Läderach & Raible, 2013) at each longitude (this sentence is repeated).

$$Q(\phi) = Q_{\max}\, e^{-\left\{\frac{(\phi-\phi_{\max})^2}{2\sigma_Q^2}\right\}} \tag{2}$$

where $Q(\phi)$ = meridonal humidity field at each longitude; $\phi_{\max}$ = meridional location of the specific humidity field at a given longitude; $Q_{\max}$ = specific humidity maximum value; σ_Q^2 = meridonal variance of specific humidity.

To fit the Gaussian function, the data are transformed, that is we take algorithm of Eq. (2), which is justified as specific humidity or refractivity is a positive quantity. The transformation reduces the problem to fit a parabola and lead to a linearized from (linear in the parameters), namely,

$$Y = f(\phi) = \ln Q(\phi)$$
$$\ln\phi_{\max} - \frac{1}{2\sigma_Q^2}.\phi^2 + 2\frac{1}{2\sigma_Q^2}\phi_{\max}\phi - \frac{1}{2\sigma_Q^2}\phi^2{}_{\max} \tag{3}$$

For each longitude, Eq. (3) can be expressed as

$$Y = f(\phi) = a.\phi^2 + b.\phi + c \tag{4}$$

where a, b, and c represent the unknown parameters estimated through the least-square fit that minimizes the deviations between

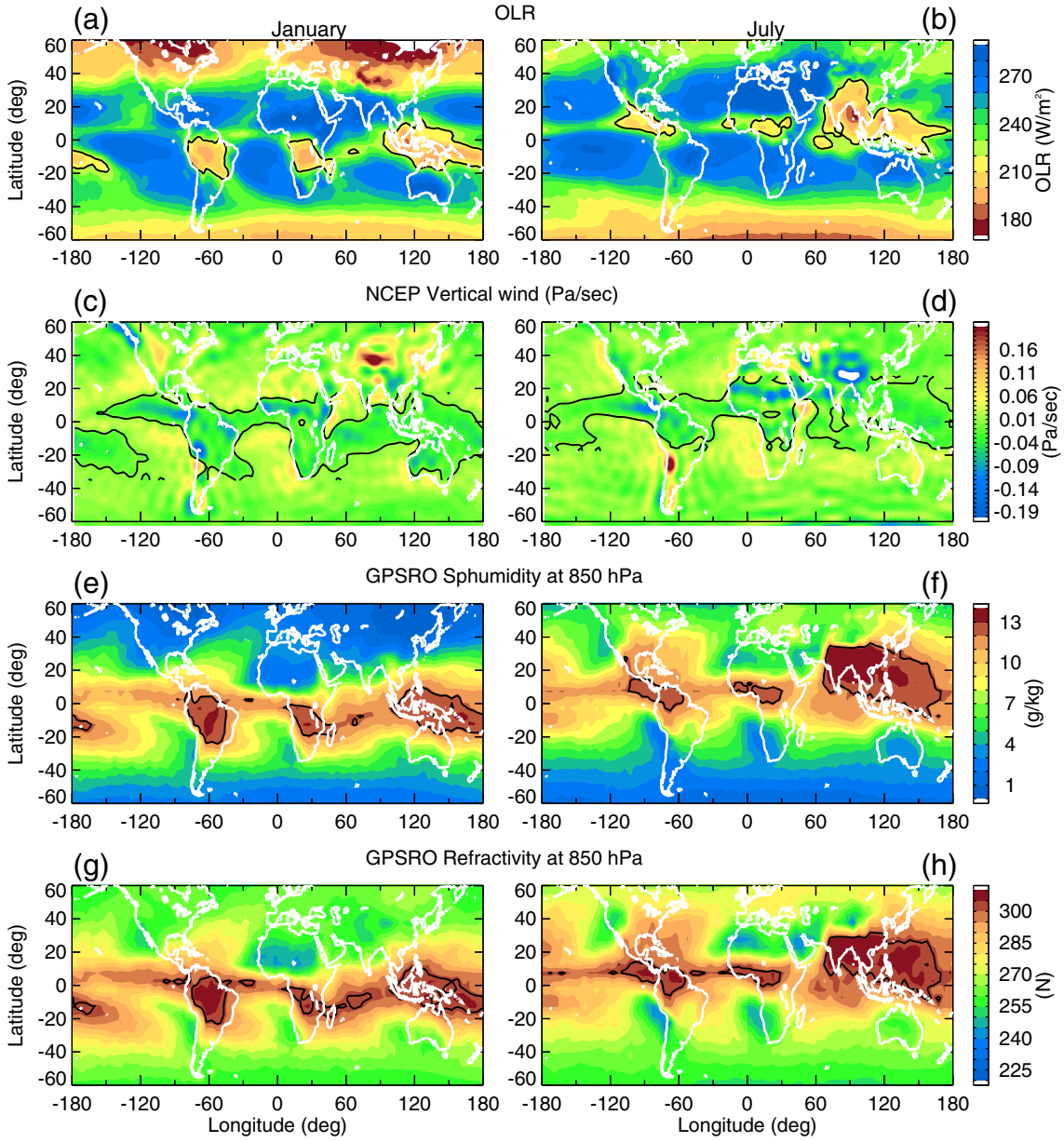

Fig. 1. Global distribution of outgoing long-wave radiation (OLR) (a, b), vertical wind (c, d), specific humidity (e, f), and refractivity (g, h) averaged from 2002 to 2013 during January (left panels) and July (right panels) at 850 hPa. The black contour line illustrates the 200–220 W/m^2 for OLR, vertical wind at 0 m/s, 10–12 g/kg for specific humidity and 300–320 N units for refractivity.

the data and the Gaussian function. The least-square fit was applied for each longitude (Wilks, 2006).

$$Y = \begin{pmatrix} y_1 \\ y_2 \\ . \\ . \\ y_n \end{pmatrix};\ X = \begin{pmatrix} \phi_0^2 & \phi_0 & 1 \\ \phi_1^2 & \phi_1 & 1 \\ . & . & . \\ . & . & . \\ \phi_n^2 & \phi_n & 1 \end{pmatrix};\ Z = \begin{pmatrix} a \\ b \\ c \end{pmatrix} \tag{5}$$

The general linear equation of the type $Y = XZ + e$. Y is a vector of trait values, Z is a vector of unknown parameters to be estimated, X is matrix of values, and e is a random vector whose components are independent and identically distributed with an unknown distribution (i.e., with zero mean and constant variance). By solving the system of normal equations in a least-square sense, the parameters a, b, and c are obtained.

$$Z = \left(X^T X\right)^{-1} X^T Y \tag{6}$$

where X and Y are defined as above, X^T indicates the transpose matrix of X, $(X^T X)^{-1}$ indicates the inverse of $(X^T X)$, and Z is the vector of regression coefficient estimates, one for each specific humidity or refractivity,

$$Z = \left(X^T W X\right)^{-1} w X^T Y \tag{7}$$

where w is the weight, which is applied to restrict the meridonal location of the humidity maximum to a certain extent around the equator. A weight is applied to the specific humidity Q and to each equation of the linear system of the regression according to

$$w_{i,i} = \cos^p(k.\phi_i) \tag{8}$$

where $w_{i,i}$ are the diagonal elements of the weight matrix 'w'.

The parameters $0 \le k \le 1$ and $p = 1, 2, \ldots$, determine how strongly the weight decreases with latitude ϕ_i and i denotes the index of the latitude vector. The two weight parameters introduce a possibility to tune the method. Further, the described weight decreases the contribution of the points far away from the maximum and reduces problems arising from potential secondary maxima in higher latitudes.

Once the linearized parameters are estimated, the back transform parameters are given by

$$Q_{\max} = e^{\left(c - \frac{b^2}{4a}\right)} \tag{9}$$

$$\phi_{\max} = -\frac{b}{2a} \tag{10}$$

$$\sigma_Q^2 = \frac{1}{2a}. \tag{11}$$

The zonal mean specific humidity or refractivity maximum is significantly dependent on the weight factor k, particularly during the NH summer, where the maximum location moves far from the equator. Therefore, we performed sensitivity analysis to test the dependence of the refractivity on the weight factor by assigning different values for k. Results indicate that $k = 0.95$ is appropriate to match with the mean specific humidity or refractivity maximum. Thus, further results are presented for the weight factor $k = 0.9$.

4. Results

Before going into the results, it is necessary to verify whether GPSRO refractivity shows a similar ITCZ structure as that of the OLR and specific humidity. Fig. 1(a) and (b) show the distribution of OLR observed during January and July averaged from 2002 to 2013, respectively. The black contour lines indicate the OLR values in the range of 200–220 W/m^2, which represents the deep convective region. The daily mean OLR is an indicator of the mean status of tropical convection. Observationally, the location of the ITCZ can be identified by the minimum in OLR values. OLR shows that the ITCZ is a meandering narrow band of cloudiness close to the equator. As discussed in the introduction section, an alternative method for the identification of the ITCZ is from convergence of winds (Žagar et al., 2011; Zheng et al., 1997), which is later related to vertical wind. Therefore, we plotted the vertical wind obtained from NCEP reanalysis data at 850 hPa as shown in Fig. 1c and d during the months of January and July. The vertical wind clearly shows the ITCZ location, which is similar to that of OLR. The ITCZ residing near the equator during the month of July over the western Pacific and Indian monsoon region is noticed. Similar features are observed in both specific humidity (1e and 1f) and refractivity (1g and 1h) obtained from GPSRO averaged during the same period during these two months at 850 hPa as that of OLR. The contour lines correspond to specific humidity in the range of 10–12 g/kg. Note that water vapor is retrieved from GPSRO satellite using a 1D variational method by taking the nearest temperature as an initial guess. The specific humidity profiles from GPSRO data below 1.4 km are affected by the negative bias. Therefore, only data from 850 hPa is considered. The refractivity from GPSRO data is a direct product and valid from surface to 40 km. The contour line in refractivity corresponds to maximum values in the range of 280–300N units. The central location of ITCZ from refractivity compares well with the other traditional methods. We applied the Gaussian fit to both specific humidity and refractivity to identify the ITCZ at each longitude.

The method based on monthly mean specific humidity and refractivity at 850 hPa is verified during January and July. Fig. 2 depicts the weighted zonal distribution of specific humidity and refractivity from

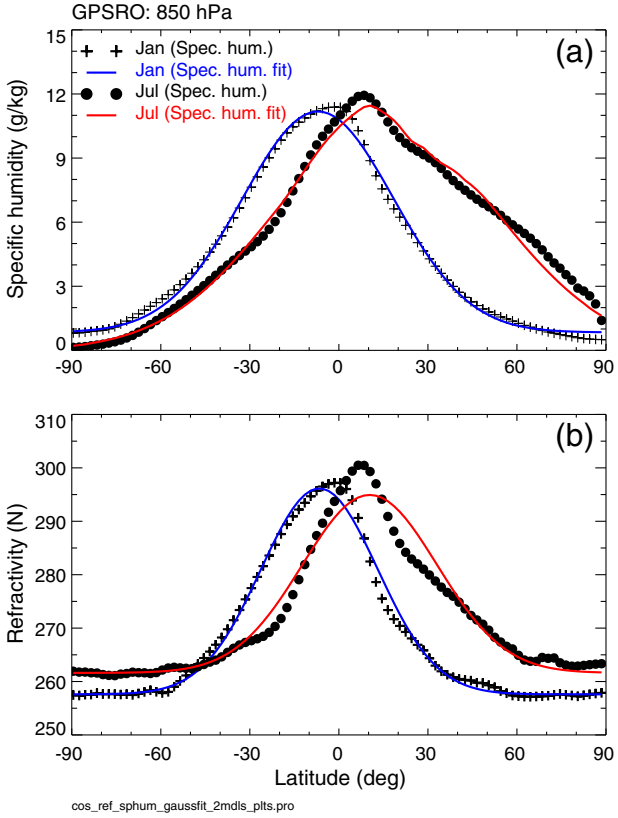

Fig. 2. Zonal mean distribution of (a) specific humidity and (b) refractivity observed during January and July averaged over the period of 2002–2013 at 850 hPa. Thick lines show the Gaussian fit.

the year 2002–2013. The resulting Gaussian fit for January and July are also shown in the figure. The specific humidity and refractivity show a similar distribution reaching the maximum at the equator during the winter and shifting toward the north (7°N) during July. However, during the month of July, there is a slight deviation in the northern latitudes. The mean maximum location obtained from refractivity from 2002 to 2013 during January and July is shown is Fig. 2(b). During January, the maximum location shifts to SH around 5°S, whereas during July it shifts 18°N. These results confirm that this method is useful for the identification of the ITCZ from refractivity data.

The mean shape and interannual variability of the ITCZ as identified from the refractivity data are shown in Fig. 3. Fig. 3a shows the mean location of maximum refractivity from 2002 to 2013 during July and January. Cross lines show the area considered for estimating the refractivity maximum for both months. The mean distribution of ITCZ shows a clear migration during the NH summer and winter months. During January, the ITCZ is located around 5°S, whereas it is around 12°N during July. Over the global oceanic regions, the ITCZ location shifts by ~20° between July and January. Although the primary focus of this paper is ITCZ identification, the year-to-year variability is also explored. Apart from the regular seasonal variations, the ITCZ undergoes interannual fluctuations in its position and intensity. Fig. 3b illustrates the interannual variability of ITCZ from GPSRO data during the months of July and January averaged from 2002 to 2013 (12 years of data). Nearly a 5° shift in the

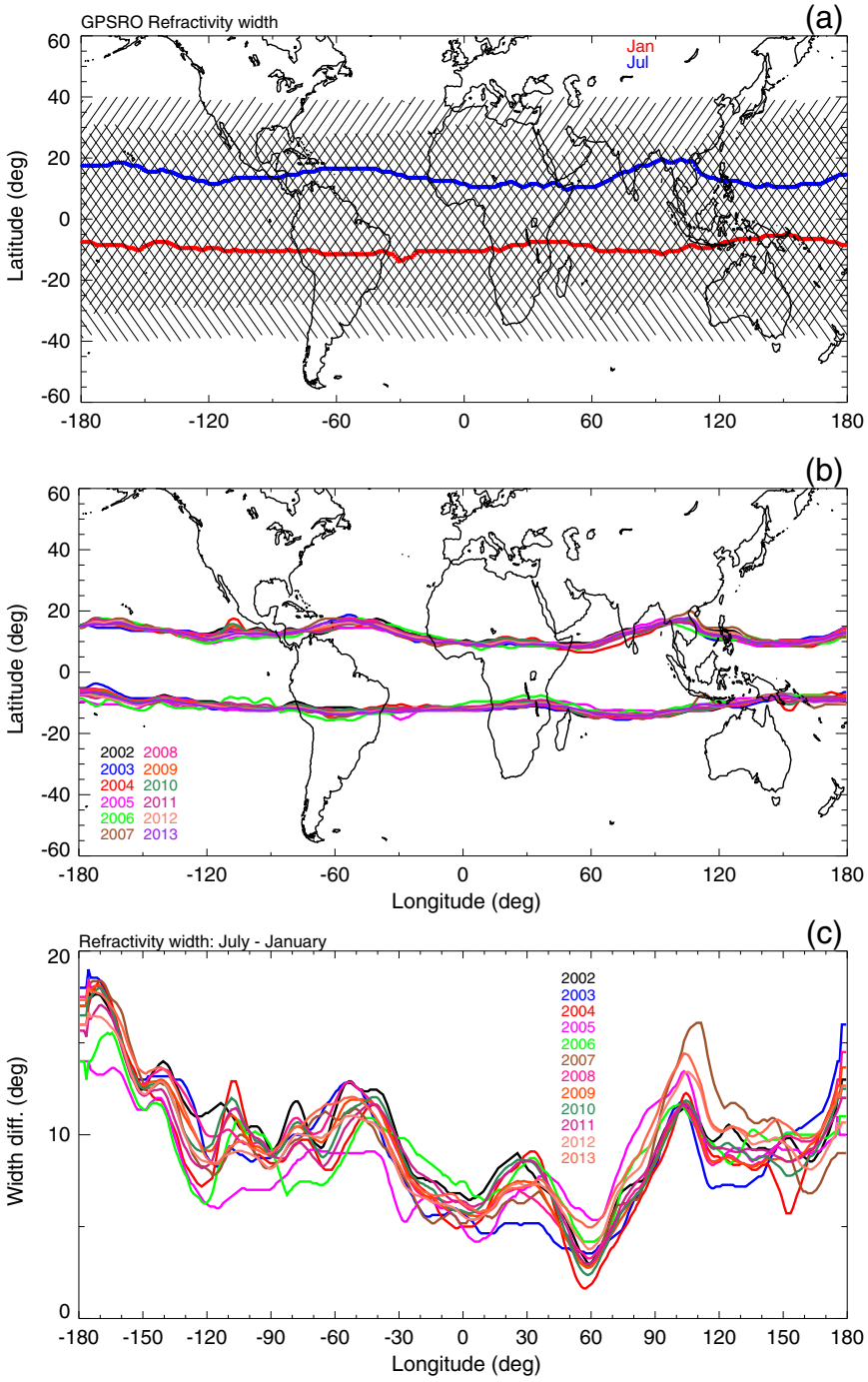

Fig. 3. (a) Estimated mean location of ITCZ during July (blue) and January (red) from GPSRO refractivity data integrated over 2002–3013. The shaded area represents the width of the Gaussian fit. (b) Interannual variability of ITCZ from 12 years of refractivity data observed during the month of July(northern hemisphere) and January(southern hemisphere), and (c) difference between July and January.

interannual variability is observed. Fig. 3c illustrates the interannual variability difference between July and January months of each year. Note that during the years 2004 and 2006, a larger variability is observed in comparison to other years. The major source for interannual variability is represented with respect to El Niño Southern Oscillation (ENSO). This will be the focus of a separate study.

Fig. 4 shows the climatology of the ITCZ derived from refractivity for four different seasons superimposed on the distribution of refractivity at 850 hPa. The main features of the ITCZ are clearly observed in refractivity. The seasonal changes of the ITCZ are noticed during its migration from NH winter to NH summer. The seasonal variability of the ITCZ varies largely over different tropical domains. The ITCZ over the eastern Pacific and Atlantic does not move much, whereas over the western Pacific and Indian Ocean, it shows large variability. The ITCZ over the land (e.g., Africa and South America) follows the annual march of the sun. The annual cycle of the ITCZ over Africa shows a migration pattern that has a nearly sinusoidal nature. During summer, the ITCZ overlies in oceanic counterparts to the east and west.

Another dramatic seasonal change associated with the ITCZ occurs in the Indian Ocean region during the Asian summer monsoon. The seasonal migration of ITCZ depends on the tropical sea surface temperatures (SST). For example, due to upwelling, the SST in central pacific region is cooler than that away from the equator on both sides. Because convection favors the warms SSTs, the ITCZ does not stay at the equator but jumps from one hemisphere to the other. Bjerknes (1969) discussed the relation between the ITCZ location and warm SST. Over the Indian Ocean and western Pacific regions, where maximum SST is at the equator, the ITCZ still prefers latitudes off the equator. Monsoon circulations play an important role in the abrupt seasonal migration of the ITCZ in the two regions. The migration of ITCZ coincides with the onset timings of the monsoon. Waliser and Gautier (1993) showed the ITCZ climatology by using a cold cloud threshold of the seasonal average to determine the signatures of the mean convergence zone that describes the ITCZ in Pacific region. Our results are in general agreement with these previous studies; however, our results show the seasonal migration of the ITCZ all over the globe. The location of the ITCZ is identified from refractivity in all seasons. Another important aspect of the analysis is that the estimated location resembles in most of the parts with the common definitions of the ITCZ. In contrast to the other existing ITCZ detection methods, like wind based method (Žagar et al., 2011), this method identifies the maximum in refractivity at each longitude. Seasonal deviation occurs in the eastern Pacific during the post-monsoon season, when the ITCZ occasionally separates into two zones of convection straddling the equator. The maximum intensity clearly identified at double-peak structure especially over the eastern Pacific region and is shown in cross symbols in Fig. 4. As in Fig. 4 over the eastern Pacific region, only the maximum intensity of the band is shown. During winter particularly over the eastern Pacific region, the detection of ITCZ becomes difficult due to the double structure of ITCZ. This new method allows for one maximum only, therefore the position of the ITCZ is not estimated properly in the longitude band of 160–120°W. A weaker double structure is found in the southwestern Atlantic, which slightly shifts the maximum in refractivity toward the south. It is noted that this pattern influences the estimation of the width and location of the refractivity distribution. Thus, the results have to be interpreted with caution during the winter especially over the eastern Pacific region. The maximum threshold values obtained from the climatology of refractivity are in the range of 280–300 N units.

The pattern of the ITCZ is seen in several meteorological parameters from the surface to the upper troposphere. Most of the upper troposphere and lower stratospheric clouds can be observed in the band of the ITCZ. For example, deep convective clouds comprise about 40–45% of total cloud signal in ITCZ (Gu & Zhang, 2002). The tropical tropopause layer (TTL) between about 14 and 18 km (Sherwood & Dessler, 2001) is the important transition layer between the convectively dominated tropical troposphere and the radiatively controlled stratosphere (Highwood & Hoskins, 1998). It accounts for much of the air entering the stratosphere from the troposphere. Due to limitations in the data sets resolution, it was very difficult to locate the ITCZ at higher altitudes. Therefore, by using high-resolution refractivity, we attempted to show the vertical variability of the ITCZ from surface to 100 hPa.

Fig. 5 shows the mean location of the ITCZ at six different pressure levels (850, 700, 500, 300, 200, 100 hPa) during January and July averaged over 12 years. A larger variability in ITCZ can be observed during the month of July than during the month of January. During the month of July, the ITCZ is located near the equator. As we move from surface to higher altitudes the ITCZ moves further to the north of the equator. A large latitudinal difference is noticed between the 850 hPa and other levels. The latitudinal difference becomes larger when we move from the Indian region to the western Pacific region between the surface and higher levels. A larger variability is found at the 700 and 500 hPa levels when compared to other levels. The variability of the ITCZ is different at different levels with respect to the longitude. The ITCZ at 700 hPa shows a large variability over the land region of Northern America and the African region, whereas a large variability is found over the Arabian Peninsula at 500 hPa. No such significant

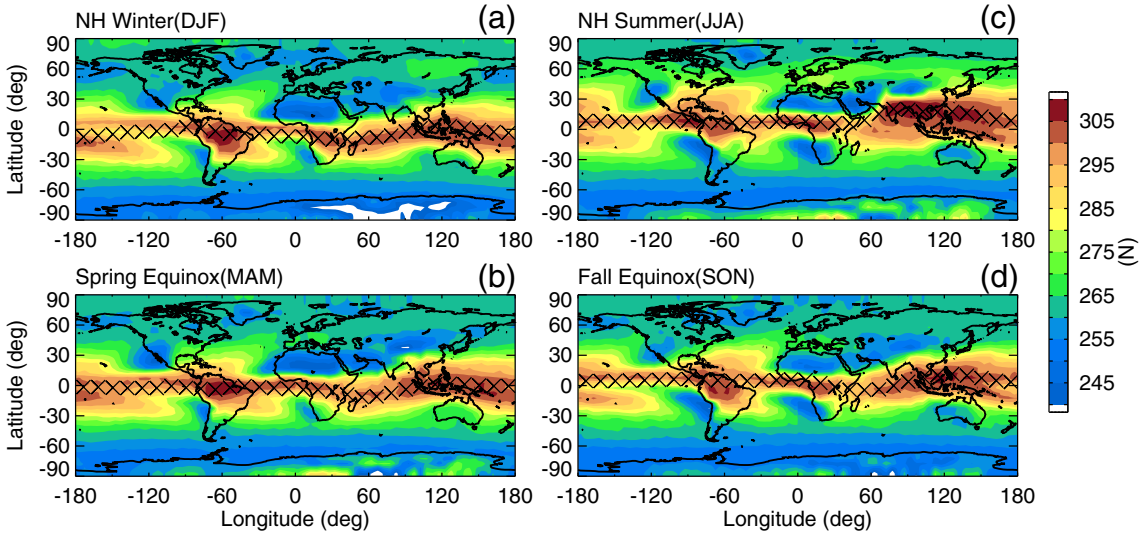

Fig. 4. Global distribution of GPS RO refractivity observed during different seasons integrated for 12 years with 2° × 2° latitude and longitude grid at 850 hPa. The stippled area indicates the ITCZ location estimated from the Gaussian distribution of refractivity maximum with a 99% threshold.

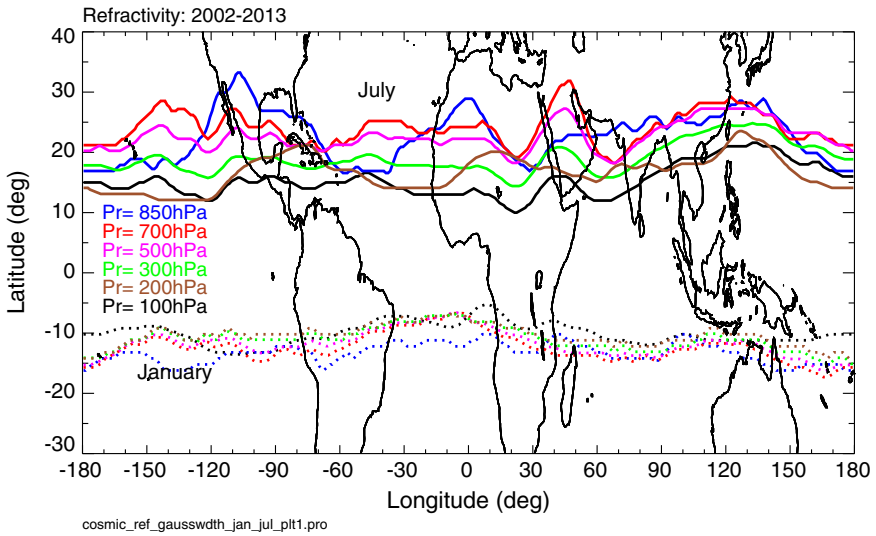

Fig. 5. ITCZ variation observed at different pressure levels using GPS RO refractivity during January (dotted lines) and July (thick lines) averaged from 2002 to 2013.

variability is observed during January at different levels. Hu, Li, and Liu (2007) investigated the vertical extent of Hadley cell and found similar results at higher altitudes (500 and 300 hPa). The ITCZ at all pressure levels is confined to one latitudinal band. This suggests that the variability of the ITCZ is more significant during the NH summer than during the NH winter season.

5. Discussion and conclusions

This study has demonstrated the strong potential for identification of the ITCZ from GPSRO refractivity data. Refractivity shows a smooth distribution of the ITCZ over the different latitudes, which allows the identification of the ITCZ more precisely than other variables like precipitation and vertical wind. Therefore, this new method is very promising in terms of the modeling of the spatial distribution of the ITCZ. Results show that global ITCZ presents a strong abrupt seasonal migration from NH summer to NH winter. A detailed analysis shows that abrupt migration in the NH winter mainly arises from cross equatorial jumps of regional ITCZ over Oceanic domains such as Indian Ocean, western Pacific, and that the second one is due to the contribution from the western and central Pacific and South America. Regional ITCZ over the Africa, eastern Pacific, and Atlantic domains does not show any abrupt migration. Our results compare well with the previous studies by Dima and Wallace (2003) and Hu et al. (2007). This method can be used for the verification of coupled climate models and can help in understanding the physical processes associated with the ITCZ. The most notable feature is the vertical variability in the ITCZ. During July, the large difference in latitudinal variation is observed between 850 hPa and other levels of the ITCZ. Lower levels show more variability than compared to higher levels during the July month. The ITCZ vertical variations are more during July than compared to January. This method would lead to better understanding the factors controlling the seasonal variability of precipitation over land regions, which are associated with the ITCZ. Finally, we conclude that, the new method estimates the ITCZ locations are consistent with other parameters like specific humidity from the same data and independent OLR data. This method is applicable to locate ITCZ at each longitude and reveals the local characteristics as well. As a result, this method can gain insights into the identification of the ITCZ with high spatiotemporal resolution. The estimated width span varies between $\pm 25°$ in both the observations. The maximum humidity detection is rather difficult in NH winter, because the double-peak structure of the distribution over the Pacific Ocean. The double ITCZ structure during NH winter makes it critical to identify the exact location of the ITCZ. In summary, the results of this study clearly show the identification of the ITCZ. Thus, it is possible to monitor the ITCZ in all-weather condition throughout the globe using GPSRO measurements.

Note that there are better precision data like the Tropical Rainfall Measuring Mission (TRMM), which provides near real-time precipitation data at a much higher resolution ($0.25° \times 0.25°$), compared to the GPSRO data used in this study ($2° \times 2°$). However, these data are not useful for knowing the vertical extent of ITCZ like GPSRO. Further, the current COSMIC mission may not provide a large sample of data in the tropical latitudes. However, GPSRO data from Radio Occultation Sounder for Atmosphere (ROSA) onboard Megha Tropiques satellite is yet to be released. It has large potential to monitor the ITCZ on day-to-day basis as it is in low inclination (23°) orbit. The upcoming new COSMIC-II with six low Earth orbit satellites in 2016 and another six satellites in 2018 will provides 10 times more coverage, i.e., ~10,000 soundings per day than existing COSMIC satellite especially in the tropical region. Such high-density profiles would be useful for better understanding of spatial and temporal evolution of the ITCZ and monitoring of climate changes associated with the ITCZ.

Acknowledgments

The authors would like to thank the Data Analysis and Archive Center (CDAAC) for providing the COSMIC GPSRO data used in this study. The authors would like to thank the Editor Dr. Marvin Bauer, and three anonymous reviewers whose comments helped considerably in improving the quality of this paper.

References

Anthes, R. A., Ector, D., Hunt, D. C., Kuo, Y-H., Rocken, C., Schreiner, W. S., et al. (2008). The COSMIC/FORMOSAT-3 mission early results. *Bulletin of the American Meteorological Society*, *89*(3), 313–333. http://dx.doi.org/10.1175/BAMS-89-3-313.

Bain, C. L., Paz, J. D., Kramer, J., Magnusdottir, G., Smyth, P., Stern, H., et al. (2010). Detecting the ITCZ in instantaneous satellite data using spatial-temporal statistical modeling: ITCZ climatology in the east Pacific. *Journal of Climate*. http://dx.doi.org/10.1175/2010JCL13716.1.

Basha, G., & Ratnam, M. V. (2009). Identification of atmospheric boundary layer height over a tropical station using high resolution radiosonde refractivity profiles: Comparison with GPS radio occultation measurements. *Journal of Geophysical Research-Atmospheres*, *114*, D16101. http://dx.doi.org/10.1029/2008JD011692.

Bean, B. R., & Dutton, E. J. (1968). *Radio Meteorology*. Dover: Dover Publications, 435.

Bjerknes, J. (1969). Atmospheric teleconnections from the equatorial Pacific. *Monthly Weather Review*, *97*, 163–172.

Chang, C. P. (1970). Westward propagating cloud patterns in the tropical Pacific as seen from time-composite satellite photographics. *Journal of Atmospheric Science*, *27*, 313–322.

Dima, M. Ioana, & Wallace, John M. (2003). On the seasonality of the Hadley cell. *Journal of Atmospheric Science*, *60*, 1522–1527. http://dx.doi.org/10.1175/1520-0469(2003)060<1522:OTSOTH>2.0.CO;2.

Gu, G., & Zhang, C. (2002). Cloud components of the Intertropical Convergence Zone. *Journal of Geophysical Research-Atmospheres*, *107*(D21), 4565. http://dx.doi.org/10.1029/2002JD002089.

Healy, S. B., & Eyre, J. R. (2000). Retrieving temperature, water vapour and surface pressure information from refractivity-index profiles derived by radio occultation: A simulation study. *Quarterly Journal of the Royal Meteorological Society*, *126*, 1661–1683. http://dx.doi.org/10.1002/qj.49712656606.

Highwood, E. J., & Hoskins, B. J. (1998). The tropical tropopause. *Quarterly Journal of the Royal Meteorological Society*, *124*, 1579–1604.

Holton, J. R., Wallace, J. M., & Young, J. A. (1971). On boundary layer dynamics and the ITCZ. *Journal of Atmospheric Science*, *28*(2), 275–280.

Hu, Y., Li, D., & Liu, J. (2007). Abrupt seasonal variation of the ITCZ and the Hadley circulation. *Geophysical Research Letters*, *34*, L18814. http://dx.doi.org/10.1029/2007GL030950.

Kishore, P., Ratnam, M. V., Namboothiri, S. P., Velicogna, I., Basha, G., Jiang, J. H., et al. (2011). Global (50S-50 N) distribution of water vapor observed by COSMIC GPS RO: Comparison with GPS radiosonde, NCEP, ERA-Interim, and JRA-25 reanalysis data sets. *Journal of Atmosphere Solar Terrestrial Physics*, *73*(13), 1849–1860. http://dx.doi.org/10.1016/j.jastp.2011.04.017.

Kursinski, E. R., Hajj, G. A., Hardy, K. R., Schofield, J. T., & Linfield, R. (1997). Observing Earth's atmosphere with radio occultation measurements. *Journal of Geophysical Research-Atmospheres*, *102*, 23,429–23,465.

Läderach, A., & Raible, C. C. (2013). Lower-tropospheric humidity: Climatology, trends and the relation to the ITCZ. *Tellus A*, *65*, 20413. http://dx.doi.org/10.3402/tellusa.v65i0.20413.

Li, G., & Xie, S. -P. (2014). Tropical biases in CMIP5 multimodel ensemble: The excessive equatorial Pacific cold tongue and double ITCZ problems. *Journal of Climate*, *27*, 1765–1780.

Magnusdottir, G., & Wang, C. C. (2008). Intertropical convergence zones during the active season in daily data. *Journal of Atmospheric Science*, *65*, 2861–2876.

Nicholson, S. E. (2009). A revised picture of the structure of the monsoon and land ITCZ over West Africa. *Climate Dynamics*, *32*, 1155–1171. http://dx.doi.org/10.1007/s00382-008-0514-3.

Rao, D. N., Ratnam, M. V., Mehta, Sanjay, Nath, Debashis, Basha, G., Jagannadha Rao, V. V. M., et al. (2009). Validation of the COSMIC radio occultation data over gadanki (13. 48°N, 79.2°E): A tropical region. *Terrestrial Journal of Atmospheric Oceanic Science*, *20*, 59–70. http://dx.doi.org/10.3319/TAO.2008.01.23.01(F3C).

Ratnam, M. V., & Basha, G. (2010). A robust method to determine global distribution of atmospheric boundary layer top from COSMIC GPS RO measurements. *Atmospheric Science Letters*, *11*, 216–222. http://dx.doi.org/10.1002/asl.277.

Ratnam, M. V., Basha, G., Krishna Murthy, B. V., & Jayaraman, A. (2014). Relative humidity distribution from SAPHIR experiment on board Megha-Tropiques satellite mission: Comparison with global radiosonde and other satellite and reanalysis data sets. *Journal of Geophysical Research-Atmospheres*, *118*. http://dx.doi.org/10.1002/jgrd.50699.

Reed, R. (1970). Structure and characteristics of easterly waves in the equatorial western Pacific during July–August 1967. *Proceedings of Symposium on Tropical Meteorology. EII*. (pp. 1–8).

Sherwood, S. C., & Dessler, A. E. (2001). A model for transport across the tropical tropopause. *Journal of Atmospheric Science*, *58*, 765–779.

Sokolovskiy, S. V. (2001). Modeling and inverting radio occultation signals in the moist troposphere. *Radio Science*, *36*, 441–458.

Thayer, G. G. (1974). An improved equation for radio refractive index of air. *Radio Science*, *9*, 803–807. http://dx.doi.org/10.1029/RS009i010p00803.

Vergados, P., Mannucci, A. J., & Su, H. (2013). A validation study for GPS radio occultation data with moist thermodynamic structure of tropical cyclone. *Journal of Geophysical Research-Atmospheres*, *118*, 9401–9413. http://dx.doi.org/10.1002/jgrd.50698.

Waliser, D. E., & Gautier, C. (1993). A satellite derived climatology of the ITCZ. *Journal of Climate*, *6*, 2162–2174.

Waliser, D. E., Groham, N. E., & Gautier, C. (1993). Comparison of the highly reflective cloud and outgoing longwave radiation datasets for use in estimating tropical deep convection. *Journal of Climate*, *6*, 331–353.

Wang, B. R., Liu, X. Y., & Wang, J. K. (2013). Assessment of COSMIC radio occultation retrieval product using global radiosonde data. *Atmospheric Measurements and Techniques*, *6*, 1073–1083. http://dx.doi.org/10.5194/amt-6-1073-2013.

Wickert, J., Reigber, C., Beyerle, G., Koenig, R., Marquardt, C., Schmidt, T., et al. (2001). Atmosphere sounding by GPS radio occultation: First results from CHAMP. *Geophysical Research Letters*, *28*, 3263–3266.

Wilks, D. (2006). Statistical methods in the atmospheric sciences. (2nd ed.). *International Geophysics Series*, *91*, . San Diego: Academic Press.

Žagar, N., Skok, G., & Tribbia, J. (2011). Climatology of the ITCZ derived from ERA interim reanalysis. *Journal of Geophysical Research-Atmospheres*, *116*, D15103. http://dx.doi.org/10.1029/2011JD015695.

Zhang, C. (1993). On the annual cycle in highest clouds in the tropics. *Journal of Climate*, *6*, 1987–1990.

Zheng, Q., Yan, X. -H., Liu, W. T., Tang, W., & Kurz, D. (1997). Seasonal and interannual variability of atmospheric convergence zones in the tropical Pacific observed with ERS-1 scatterometer. *Geophysical Research Letters*, *24*(3), 261–263.